JOURNAL OF MAGNETIC RESONANCE 77, 274–293 (1988)

Iterative Schemes for Bilinear Operators; Application to Spin Decoupling

A. J. SHAKA, C. J. LEE, AND A. PINES

Department of Chemistry, University of California, Berkeley, California 94720, and Materials and Chemical Sciences Division, Lawrence Berkeley Laboratory, Berkeley, California 94720

Received June 23, 1987; revised August 13, 1987

We extend the idea of iterative schemes from the single-spin to the two-spin case. As an application we derive a new series of broadband heteronuclear decoupling sequences, called the DIPSI sequences. They give better *quality* decoupling of protons from carbon-13 than previous sequences like WALTZ-16 when there is scalar coupling among the protons. In the absence of such coupling, the DIPSI sequences offer the same high standard of performance as WALTZ-16, but over somewhat smaller bandwidths.

INTRODUCTION

Current schemes for broadband heteronuclear decoupling in NMR spectroscopy of isotropic liquids employ periodic sequences of radiofrequency pulses derived according to an iterative recipe (*1–5*). The idea behind these schemes rests on the observation (*6*) that, neglecting any homonuclear interactions among the irradiated (I) or observed (S) spins, decoupling can be analyzed by considering only the behavior of an isolated ensemble of I spins under the influence of a single period of the pulse sequence. To decouple I from S over a certain bandwidth, it is sufficient to design a propagator for the I spins which is nearly constant over the same bandwidth. In practice, and for a number of good reasons, iterative schemes all attempt to implement a propagator that is the identity operator over the desired bandwidth, corresponding to a Hamiltonian represented by the null operator. Almost all progress has centered on the simplest model of two (otherwise isolated) weakly coupled spins $I = S = \frac{1}{2}$; the resulting sequences work equally well for arbitrary spin nuclei in the absence of any quadrupolar interactions, however. We shall refer to this situation as the "single-spin case," as only a single I spin is involved.

The simple single-spin model can be expanded to a two-spin model by introducing a second I spin. The spins I_1 and I_2 are scalar coupled and I_1 is coupled to the heteronucleus S, but I_2 is not coupled to S. This last assumption ensures that any changes in the S-spin spectrum result only from the coupling between the I spins and not simply from an additional coupling between I_2 and S. In the practical case, the S spin will be carbon-13 and the I spins will be protons. The only role of S is, depending on its spin state, to augment or retard the local field experienced by I_1, giving it a slightly different chemical shift. Accordingly, most of our development will concentrate on the behavior of the two I spins under modulated irradiation.

In the presence of homonuclear scalar coupling among the I spins, it is not possible

0022-2364/88 $3.00

to produce the identity operator unless the pulse sequence pairwise decouples each I spin from every other. Such homonuclear decoupling in the case of arbitrary tightly coupled proton spin systems including large resonance offset effects appears to be an unrealistic goal at this time, so it becomes necessary to consider designing some other offset-independent propagator for the I spins. The natural choice for such a propagator corresponds to a Hamiltonian containing only the scalar interactions $\mathbf{I}_k \cdot \mathbf{I}_l$ between each pair of I spins.

Here we demonstrate that it is possible to design such a propagator for the case of two coupled spins $I = \frac{1}{2}$. Our sequences can be considered to be a generalization of the MLEV (*1*) and Waugh (*2*) schemes: in addition to averaging the terms involving linear spin operators to nearly zero, we also average all bilinear combinations to nearly zero except for the pure scalar $\mathbf{I}_1 \cdot \mathbf{I}_2$. As a result, the new sequences perform better than WALTZ-16 when there are inequivalent coupled I spins present. They may also have applications for the decoupling of spins $I = 1$ in anisotropic phase (*7*) and broadband homonuclear cross-polarization experiments (*8*). The theory needed to describe the removal of all linear and bilinear terms relates very closely to the theory of multiple-pulse experiments in zero field (*9*).

We begin by describing the design of composite pulses capable of removing the influence of I-spin resonance offsets from the effective Hamiltonian while leaving the scalar interaction largely unperturbed. In contrast to some previous discussions of this subject (*8, 10, 11*) and in agreement with a recent communication concerning broadband homonuclear cross polarization (*12*) and a paper describing the effect of homonuclear coupling on broadband heteronuclear decoupling (*13*), it is found that windowless sequences of RF pulses can produce an effective Hamiltonian containing a combination of bilinear operators $I_{1\alpha}I_{2\beta}$ ($\alpha, \beta = x, y, z$). In particular, the coefficients of $I_{1x}I_{2x}$, $I_{1y}I_{2y}$, and $I_{1z}I_{2z}$ can become unequal; that is, the scalar interaction becomes nonscalar under the influence of the modulated RF field. This behavior is markedly different than that discussed by Braunschweiler and Ernst (*8*) who assumed the δ-pulse limit in calculating the zeroth-order average Hamiltonian for their sequences: in that case no nonscalar behavior is predicted.

Given a composite pulse that largely removes resonance offset effects, we next show how to combine such pulses into sequences that, to first order, cancel all linear terms and bilinear cross terms. The initial sequences can be based on either composite 90° or 180° pulses combined into short cycles, as in the case of single I-spin sequences like MLEV or WALTZ (*1, 3*). We show by calculation that, over their somewhat smaller operational bandwidths, these new decoupling sequences can outperform previous sequences when there is scalar coupling among the I spins, while still maintaining the same high standard of performance in the absence of such coupling. The best candidates for proton decoupling, based on composite 180° pulses, are insensitive to spectrometer phase misadjustments or pulse miscalibration and perform well in practice, as we demonstrate by experiment. Finally, we close by discussing several closely related experiments and the advantages of bilinear averaging.

PHASE-ALTERNATING COMPOSITE PULSES IN THE PRESENCE OF SCALAR COUPLING

We consider a Hamiltonian for two coupled spins I_1 and I_2 in which I_1 is assumed to be on resonance and I_2 is off resonance by an amount $\Delta\omega$. We apply an RF decou-

pling field ω_2 to perturb the I spins. In the usual rotating frame, the Hamiltonian during the kth pulse, of duration τ_k, can be written

$$\mathscr{H}_k = \mathscr{H}_{krf} + V \quad [1]$$

where

$$\mathscr{H}_{krf} = (-1)^k \omega_2 (I_{1x} + I_{2x}) \quad [2]$$

$$V = \Delta\omega I_{2z} + 2\pi J \mathbf{I}_1 \cdot \mathbf{I}_2. \quad [3]$$

We have assumed that each pulse is applied along the x or $-x$ axis of the rotating frame, and that its amplitude ω_2 and frequency are fixed. An earlier treatment of phase-alternating composite pulses has shown (*14*) that, providing $J = 0$, this class of composite pulses can produce a propagator at time $\tau = \Sigma_k \tau_k$ that approximates an ideal RF pulse; that is,

$$U(\tau) = \prod_k \exp(-i\tau_k \mathscr{H}_k) \approx \exp(i\alpha[I_{1x} + I_{2x}]). \quad [4]$$

The flip angle α can be selected at will; Eq. [4] is understood to be true for some range of $\Delta\omega$ values about exact resonance ($\Delta\omega = 0$) when the appropriate pulse widths τ_k are selected. We take the same approach here, but include the scalar coupling interaction in the calculation.

Using coherent averaging theory (*15*) we transform into an interaction picture dictated by $\mathscr{H}_{rf}$ and treat V as a perturbation. The propagator separates into a product

$$U(\tau) = U_{rf}(\tau) U_v(\tau), \quad [5]$$

where $U_{rf}(\tau)$ represents the ideal transformation and $U_v(\tau)$ the imperfection,

$$U_v(\tau) = T \exp\left\{-i \int \tilde{V}(t) dt\right\} \quad [6]$$

$$\tilde{V}(t) = U_{rf}(t)^{-1} V U_{rf}(t), \quad [7]$$

where T denotes time ordering. This decomposition is not an approximation. $U_v(\tau)$ is then approximated using the Magnus expansion (*16, 17*),

$$U_v(\tau) = \exp(-i\tau[V^{(0)} + V^{(1)} + V^{(2)} + \cdots]), \quad [8]$$

in which the Hermitian operators $V^{(n)}$ rapidly become insignificant provided $\omega_2 \gg |\Delta\omega|$, $|J|$ as would be the case for proton decoupling in liquids.

The terms in the expansion are well-known. The first three terms in the series are given by

$$V^{(0)} = \frac{1}{\tau} \int_0^\tau dt_1 \tilde{V}_1 \quad [9]$$

$$V^{(1)} = \frac{-i}{2\tau} \int_0^\tau dt_1 \int_0^{t_1} dt_2 [\tilde{V}_1, \tilde{V}_2] \quad [10]$$

$$V^{(2)} = \frac{-1}{6\tau} \int_0^\tau dt_1 \int_0^{t_1} dt_2 \int_0^{t_2} dt_3 [\tilde{V}_1, [\tilde{V}_2, \tilde{V}_3]] + [\tilde{V}_3, [\tilde{V}_2, \tilde{V}_1]], \quad [11]$$

where we use the shorthand $\tilde{V}_n \equiv \tilde{V}(t_n)$. Higher-order terms in the Magnus expansion are available if necessary (*18–20*). Our goal is to arrange that all terms in $\Delta\omega$ vanish, so that $U_v(\tau)$ becomes the evolution due to pure scalar coupling,

$$U_v(\tau) = \exp(-i2\pi\tau J\mathbf{I}_1 \cdot \mathbf{I}_2), \qquad [12]$$

and the Magnus expansion is useful because it quickly allows us to predict the operators that the composite pulse may produce and their dependence on $\Delta\omega$ and J.

Consider an arbitrary phase-alternating sequence of m pulses $\alpha_1\bar{\alpha}_2\alpha_3 \ldots$, the overbars representing a phase shift of π and the flip angles α_i denoting those at exact resonance. Let Δ_n be defined by

$$\Delta_n = \sum_{k=0}^{n} (-1)^k \alpha_k \qquad [13]$$

with $\alpha_0 \equiv 0$. Carrying out the integration for $V^{(0)}$ we find

$$\tau V^{(0)} = 2\pi J\tau\mathbf{I}_1 \cdot \mathbf{I}_2 + \frac{\Delta\omega}{\omega_2} \sum_{j=1}^{m} (-1)^{(j+1)}\{I_{2z}(\sin\Delta_j - \sin\Delta_{j-1}) + I_{2y}(\cos\Delta_{j-1} - \cos\Delta_j)\}. \qquad [14]$$

To zeroth order in the Magnus expansion the coupling is unaffected by the composite pulse, while the terms under the summation correspond to those for the case of a single spin. A single 2π pulse causes these terms to vanish, so for $\Delta\omega/\omega_2$ sufficiently small a pure scalar operator is produced. This limit, corresponding to coherent irradiation with an extremely intense RF field, is not sufficiently discriminating to be of interest. Accordingly, the next term in the expansion must be examined.

After a perfectly straightforward but somewhat lengthy calculation, we find the following result for $\tau V^{(1)}$,

$$\tau V^{(1)} = \frac{\Delta\omega^2}{\omega_2^2} I_{2x}[\sum_j^m a_j + \sum_{k>j}^m a_{kj}] + \frac{\Delta\omega 2\pi J}{\omega_2^2}(I_{1y}I_{2x} - I_{1x}I_{2y})[\sum_j^m b_j + \sum_{k>j}^m b_{kj}] + \frac{\Delta\omega 2\pi J}{\omega_2^2}(I_{1x}I_{2z} - I_{1z}I_{2x})[\sum_j^m c_j + \sum_{k>j}^m c_{kj}] \qquad [15]$$

with coefficients defined by

$$a_j = (-1)^j\{\alpha_j - \sin\alpha_j\} \qquad [16]$$

$$a_{kj} = (-1)^{k+j}\{\sin(\Delta_k - \Delta_j) - \sin(\Delta_{k-1} - \Delta_j) - \sin(\Delta_k - \Delta_{j-1}) + \sin(\Delta_{k-1} - \Delta_{j-1})\} \qquad [17]$$

$$b_j = 2\cos\Delta_{j-1} - 2\cos\Delta_j + (-1)^j\alpha_j(\sin\Delta_j + \sin\Delta_{j-1}) \qquad [18]$$

$$b_{kj} = (-1)^{j+1}\alpha_k(\sin\Delta_j - \sin\Delta_{j-1}) + (-1)^k\alpha_j(\sin\Delta_k - \sin\Delta_{k-1}) \qquad [19]$$

$$c_j = 2\sin\Delta_{j-1} - 2\sin\Delta_j + (-1)^{j+1}\alpha_j(\cos\Delta_j - \cos\Delta_{j-1}) \qquad [20]$$

$$c_{kj} = (-1)^j\alpha_k(\cos\Delta_j - \cos\Delta_{j-1}) + (-1)^{k+1}\alpha_j(\cos\Delta_k - \cos\Delta_{k-1}). \qquad [21]$$

To first order in the Magnus expansion the action of the composite pulse creates additional bilinear operators not present in the unperturbed Hamiltonian. These terms, especially the combination $(I_{1y}I_{2x} - I_{1x}I_{2y})$, which is invariant to π phase shifts, can introduce an offset dependence into $U(\tau)$ that interferes with proper decoupling of I from S. The above equations provide a means to eliminate or at least minimize the contribution of these unwanted operators.

To explore the deviation of $\mathbf{I}_1 \cdot \mathbf{I}_2$ from its scalar form it is necessary to calculate the contribution of the operator $V^{(2)}$ to the propagator. $V^{(2)}$ has a very complicated form, so we restrict ourselves to the assessment of the operator combinations it can produce. These are as follows: the operators I_{2z} and I_{2y} with coefficients depending on $\Delta\omega^3/\omega_2^3$, the operators $I_{1x}I_{2x}$, $I_{1y}I_{2y}$, $I_{1z}I_{2z}$, $I_{1y}I_{2z}$, and $I_{1z}I_{2y}$ with coefficients depending on $\Delta\omega^2 J/\omega_2^3$, and the operators I_{1z}, I_{2z}, I_{1y} and I_{2y} with coefficients depending on $\Delta\omega J^2/\omega_2^3$. The interesting point here is that the coefficients of $I_{1\alpha}I_{2\alpha}$, $\alpha = x, y, z$, become unequal and that linear spin operators are produced for the first spin even though it is assumed to be exactly on resonance. These rather surprising linear terms arise due to the interaction of the RF field and the spin coupling producing an additional small field on the first spin.

ELIMINATING LINEAR AND BILINEAR SPIN OPERATORS

Assume we have found a composite pulse. We now explore methods to combine these into cycles that remove all linear and bilinear spin operators except for the scalar operator $\mathbf{I}_1 \cdot \mathbf{I}_2$. We write the propagator for the pulse in the form

$$U(\tau) = U_{\mathrm{rf}}(\tau)U_{\mathrm{v}}(\tau) \qquad [22]$$

and we assume nothing about $U_{\mathrm{v}}(\tau)$ except that it can be expressed as a complex exponential of the most general two-spin Hamiltonian, a sum of the 15 possible linear and bilinear operators. The only information we require is how U_{v} transforms under RF pulses and phase shifts. As the *original* perturbation V commutes with rotations about the z axis, it follows that U_{v} is tied to the phase of the RF irradiation. If U_0 denotes the propagator that results when the first pulse of the composite is applied with RF phase $\phi = 0$ then the propagator U_ϕ that results when all phases are shifted by ϕ is simply

$$U_\phi = R_z(\phi)U_0R_z(\phi)^{-1} = U_{\mathrm{rf}\phi}U_{\mathrm{v}\phi}. \qquad [23]$$

We wish to calculate the effect of a sequence of n such composite pulses, the kth pulse being applied with relative phase ϕ_k, with no detailed knowledge of the nature of U_v. In addition, we hope to find sequences that tend to cancel out the effect of the U_v operators. To do this we reorganize the product so that the RF terms are collected on the left,

$$\begin{aligned} U_{\phi_n}U_{\phi_{n-1}}\cdots U_{\phi_1} &= U_{\mathrm{rf}\phi_n}U_{\mathrm{v}\phi_n}U_{\mathrm{rf}\phi_{n-1}}U_{\mathrm{v}\phi_{n-1}}\cdots U_{\mathrm{rf}\phi_1}U_{\mathrm{v}\phi_1} \\ &= U_{\mathrm{rf}\phi_n}U_{\mathrm{rf}\phi_{n-1}}\cdots U_{\mathrm{rf}\phi_1}\{U_{\mathrm{rf}\phi_1}^{-1}\cdots U_{\mathrm{rf}\phi_{n-1}}^{-1}\}U_{\mathrm{v}\phi_n}\{U_{\mathrm{rf}\phi_{n-1}}\cdots U_{\mathrm{rf}\phi_1}\} \\ &\qquad \cdots\{U_{\mathrm{rf}\phi_1}^{-1}\}U_{\mathrm{v}\phi_2}\{U_{\mathrm{rf}\phi_1}\}U_{\mathrm{v}\phi_1} \\ &= U_{\mathrm{rf}\phi_n}U_{\mathrm{rf}\phi_{n-1}}\cdots U_{\mathrm{rf}\phi_1}\tilde{U}_{\mathrm{v}\phi_n}\tilde{U}_{\mathrm{v}\phi_{n-1}}\cdots\tilde{U}_{\mathrm{v}\phi_1}, \end{aligned} \qquad [24]$$

where the operators $\tilde{U}_v$ are defined by

$$\tilde{U}_{v\phi_k} = \{U_{rf\phi_1}^{-1} \cdots U_{rf\phi_{k-1}}^{-1}\} U_{v\phi_k} \{U_{rf\phi_{k-1}} \cdots U_{rf\phi_1}\}. \quad [25]$$

Since all the $\tilde{U}_v$ are assumed to be small perturbations, they may be grouped into a single unitary operator by applying the Baker–Campbell–Hausdorff (BCH) formula:

$$\prod_k \exp(-iA_k) = \exp\left(-i\left\{\sum_k A_k + \frac{1}{2}\sum_{k>j}[A_k, A_j] + \cdots\right\}\right). \quad [26]$$

Equation [26] is true for arbitrary linear operators A_k, the expansion consisting of an infinite series of nested commutators. Provided all A_k are of order ϵ, the commutator is of order ϵ^2 and can be neglected, along with all higher-order terms. We assume A_1 is arbitrary and that all other A_k are related by Eqs. [23] and [25]. Finding the appropriate pulse cycle then reduces to determining the sequence of phases ϕ_k such that

$$\frac{1}{n}\sum_{k=1}^{n} A_k = 0 \quad [27]$$

for the single-spin case and

$$\frac{1}{n}\sum_{k=1}^{n} A_k = 2\pi J\tau \mathbf{I}_1 \cdot \mathbf{I}_2 \quad [28]$$

for the two-spin case. Equations [27] and [28] form one possible criterion for primitive sequences in each of these cases.

The way this cancellation works can be illustrated by the single-spin case, where the imperfections A_k can be written in the form $\epsilon_k \cdot \mathbf{I}$. Consider a sequence of four composite 180° pulses, $U\,U\,\bar{U}\,\bar{U}$, the barred states denoting a 180° phase shift of all the constituent pulses, and assume U is equivalent to an x pulse on resonance. A table can be prepared listing each operator A_k underlying the $\tilde{U}_{v\phi_k}$ for each value of k, as shown in Table 1. An even number of states is required to null the ϵ_z terms; the additional requirement that both the ϵ_x and ϵ_y terms vanish makes the minimum of four states, the origin of the MLEV-4 sequence proposed by Levitt and Freeman (*21*). Of course there are many sequences of composite 180° pulses that satisfy Eq. [27], but the MLEV-4 sequence is the shortest.

In the bilinear case the vectors ϵ_k have 15 components, reflecting all possible linear and bilinear terms. The MLEV-4 sequence cancels the linear terms ϵ_α and bilinear

TABLE 1

Cancellation of Linear Spin Operators by the Sequence $U\,U\,\bar{U}\,\bar{U}$

State	Operator		
	I_x	I_y	I_z
1	ϵ_x	ϵ_y	ϵ_z
2	ϵ_x	$-\epsilon_y$	$-\epsilon_z$
3	$-\epsilon_x$	$-\epsilon_y$	ϵ_z
4	$-\epsilon_x$	ϵ_y	$-\epsilon_z$

cross terms $\epsilon_{\alpha\beta}$ ($\alpha \neq \beta$), but fails to average the $\epsilon_{\alpha\alpha}$, as the operator $I_{1z}I_{2z}$ is invariant to 180° rotations. We considered two strategies: (1) find a composite 180° pulse that keeps the $\epsilon_{\alpha\alpha}$ nearly equal as a function of resonance offset and then use an MLEV-4 sequence to cancel all other terms; (2) devise another sequence that averages the $\epsilon_{\alpha\alpha}$ as well as cancels the other terms. The first approach has been more successful in the work described here, but we briefly describe the second to establish a clear connection between the single-spin and two-spin cases.

The averaging of the $\epsilon_{\alpha\alpha}$ requires that the number of states in the sequence be a multiple of three. With the independent requirement of four states to cancel the linear terms, a 12-state sequence seems to be required. Using only 90° (composite) pulses and 90° phase shifts three distinct sequences were found. With the shorthand X, Y, $\bar{X}$, and $\bar{Y}$ denoting (composite) 90° pulses equivalent to 90° pulses along these four axes, these can be written $(X\,Y\,\bar{X}\,Y)^3$, $(X\,Y\,X\,Y\,\bar{X}\,Y)^2$, and $(X\,Y\,X\,Y\,X\,\bar{Y})^2$. The behavior of the error terms can be examined in the same way as for the single-spin case. For example, Table 2 shows the systematic cancellation of the errors under the action of the 12-pulse sequence $(X\,Y\,\bar{X}\,Y)^3$. Since the operators $I_{1\alpha}$ and $I_{2\alpha}$ transform identically, only the former are listed. One advantage of this treatment is that we are free to substitute *any* composite 90° rotation into any of these sequences. This would not be the case if we had used the Magnus expansion alone and considered the operator V as the perturbation. In such a case a separate calculation over the entire sequence would be required each time a different composite pulse is considered. The price paid for this convenience is that the exact form of U_v must remain unspecified.

Table 2 shows both the strong and the weak points of the 12-pulse sequences. The strong point is that, to first order, a true scalar operator $\mathbf{I}_1 \cdot \mathbf{I}_2$ will be produced by such a sequence. The weak point is that the radius of convergence is poorer than MLEV-4, especially for the linear terms ϵ_α. These terms are canceled only at the end of the entire 12-pulse sequence, and all three components are mixed together along the way. The MLEV-4 sequence has a subcycle structure that cancels the ϵ_α much more effi-

TABLE 2

Cancellation of Nonscalar Spin Operators by the 12-Pulse Sequence $X\,Y\,\bar{X}\,Y\,X\,Y\,X\,\bar{Y}\,X\,Y\,\bar{X}\,Y$

State	Operator											
	I_{1x}	I_{1y}	I_{1z}	$I_{1x}I_{2y}$	$I_{1x}I_{2z}$	$I_{1y}I_{2z}$	$I_{1y}I_{2x}$	$I_{1z}I_{2x}$	$I_{1z}I_{2y}$	$I_{1x}I_{2x}$	$I_{1y}I_{2y}$	$I_{1z}I_{2z}$
1	ϵ_x	ϵ_y	ϵ_z	ϵ_{xy}	ϵ_{xz}	ϵ_{yz}	ϵ_{yx}	ϵ_{zx}	ϵ_{zy}	ϵ_{xx}	ϵ_{yy}	ϵ_{zz}
2	$-\epsilon_y$	$-\epsilon_z$	ϵ_x	ϵ_{yz}	$-\epsilon_{yx}$	$-\epsilon_{zx}$	ϵ_{zy}	$-\epsilon_{xy}$	$-\epsilon_{xz}$	ϵ_{yy}	ϵ_{zz}	ϵ_{xx}
3	ϵ_z	$-\epsilon_x$	$-\epsilon_y$	$-\epsilon_{zx}$	$-\epsilon_{zy}$	ϵ_{xy}	$-\epsilon_{xz}$	$-\epsilon_{yz}$	ϵ_{yx}	ϵ_{zz}	ϵ_{xx}	ϵ_{yy}
4	ϵ_x	$-\epsilon_y$	ϵ_z	ϵ_{xy}	$-\epsilon_{xz}$	$-\epsilon_{yz}$	ϵ_{yx}	$-\epsilon_{zx}$	$-\epsilon_{zy}$	ϵ_{xx}	ϵ_{yy}	ϵ_{zz}
5	$-\epsilon_y$	ϵ_z	$-\epsilon_x$	$-\epsilon_{yz}$	ϵ_{yx}	$-\epsilon_{zx}$	$-\epsilon_{zy}$	ϵ_{xy}	$-\epsilon_{xz}$	ϵ_{yy}	ϵ_{zz}	ϵ_{xx}
6	ϵ_z	ϵ_x	ϵ_y	ϵ_{zx}	ϵ_{zy}	ϵ_{xy}	ϵ_{xz}	ϵ_{yz}	ϵ_{yx}	ϵ_{zz}	ϵ_{xx}	ϵ_{yy}
7	ϵ_x	$-\epsilon_y$	$-\epsilon_z$	$-\epsilon_{xy}$	$-\epsilon_{xz}$	ϵ_{yz}	$-\epsilon_{yx}$	$-\epsilon_{zx}$	ϵ_{zy}	ϵ_{xx}	ϵ_{yy}	ϵ_{zz}
8	ϵ_y	ϵ_z	ϵ_x	ϵ_{yz}	ϵ_{yx}	ϵ_{zx}	ϵ_{zy}	ϵ_{xy}	ϵ_{xz}	ϵ_{yy}	ϵ_{zz}	ϵ_{xx}
9	$-\epsilon_z$	$-\epsilon_x$	ϵ_y	ϵ_{zx}	$-\epsilon_{zy}$	$-\epsilon_{xy}$	ϵ_{xz}	$-\epsilon_{yz}$	$-\epsilon_{yx}$	ϵ_{zz}	ϵ_{xx}	ϵ_{yy}
10	$-\epsilon_x$	ϵ_y	$-\epsilon_z$	$-\epsilon_{xy}$	ϵ_{xz}	$-\epsilon_{yz}$	$-\epsilon_{yx}$	ϵ_{zx}	$-\epsilon_{zy}$	ϵ_{xx}	ϵ_{yy}	ϵ_{zz}
11	ϵ_y	$-\epsilon_z$	$-\epsilon_x$	$-\epsilon_{yz}$	$-\epsilon_{yx}$	ϵ_{zx}	$-\epsilon_{zy}$	$-\epsilon_{xy}$	ϵ_{xz}	ϵ_{yy}	ϵ_{zz}	ϵ_{xx}
12	$-\epsilon_z$	ϵ_x	$-\epsilon_y$	$-\epsilon_{zx}$	ϵ_{zy}	$-\epsilon_{xy}$	$-\epsilon_{xz}$	ϵ_{yz}	$-\epsilon_{yx}$	ϵ_{zz}	ϵ_{xx}	ϵ_{yy}

ciently. We note that the opposite situation can prevail for a single spin $I = 1$ in a liquid crystal environment, due to the bilinear terms generated by the large quadrupolar interaction (*7*). In such a case, rapid cancellation of the bilinear terms could be more important. For proton decoupling in liquids, however, the resonance offset and RF inhomogeneity terms are so much larger than the proton scalar coupling that increased compensation for the latter at the expense of the former is unacceptable. As a result, we have found that sequences based on composite 180° pulses are still the method of choice.

THE S-SPIN SPECTRUM UNDER A PURE SCALAR OPERATOR

The expected form of the S-spin spectrum under periodic irradiation to the I spins has already been described in detail for the case of two coupled I spins (*13*) and also treated generally for any multilevel spin system (*22*), so we restrict ourselves to a brief summary of the conclusions relevant to our discussion. We assume stroboscopic observation of the S-spin free induction decay synchronized with the decoupler cycling rate.

The evolution operator for the joint spin system at the time t_s the first point of the S-spin free induction decay is sampled separates into a sum of commuting operators depending on the spin state of S,

$$U(t_s) = P_+ U_+(t_s) + P_- U_-(t_s), \qquad [29]$$

where

$$P_\pm = \tfrac{1}{2}(\mathbf{1} \pm S_z). \qquad [30]$$

In a rotating frame on resonance for S and assuming quadrature detection after an initial 90° pulse applied to the S spins, the S-spin signal can be calculated at any multiple of t_s using the formula

$$\begin{aligned}\langle S^-(nt_s)\rangle &= \mathrm{Tr}\{(S_x - iS_y)U^n(t_s)S_x U^{-n}(t_s)\} \\ &= \mathrm{Tr}\{U_+^n(t_s)U_-^{-n}(t_s)\}. \end{aligned} \qquad [31]$$

The unitary operators $U_\pm$ can be considered to arise from fictitious time-independent Hamiltonians $\mathscr{H}_\pm$ that would have caused the same change in the quantum states over the time t_s,

$$U_\pm(t_s) = \exp(-i\mathscr{H}_\pm t_s). \qquad [32]$$

The only difference in $\mathscr{H}_\pm$ arises from the different resonance frequency of I_1, by an amount J_{IS}. In the regime of interest, and for the sequences we consider, it is safe to assume that the eigenvectors of $\mathscr{H}_+$ and $\mathscr{H}_-$ are nearly coincident, and Eq. [31] can thus be evaluated in a basis in which both operators are diagonal. The result is

$$\langle S^-(nt_s)\rangle = \sum_{j=1}^{4} \exp(it_s(\Omega_{j+} - \Omega_{j-})), \qquad [33]$$

where $\Omega_{j\pm}$ are the jth eigenvalues of $\mathscr{H}_\pm$. In this limit, Fourier transformation of the time-domain signal of Eq. [31] gives an S-spin spectrum containing four lines of unit intensity with frequencies given by the appropriate energy difference. The eigenvalues are functions of the chemical shift of I_1, δ_1: $\Omega_j = \Omega_j(\delta_1)$. The only role of the coupling

is to give I_1 a slightly different chemical shift in each subspectrum. Since the perturbation is small, it is valid to approximate the difference by the derivative. Putting $E_{j\pm} = 2\pi\Omega_{j\pm}$ and expressing all offsets and energies in hertz, we have

$$E_{j+} - E_{j-} = E_j(\delta_1 + J_{IS}/2) - E_j(\delta_1 - J_{IS}/2) \approx J_{IS}\frac{\partial E_j}{\partial \delta_1}. \quad [34]$$

Accordingly, we can define a set of j scaling factors by

$$\lambda_j = \frac{\partial E_j}{\partial \delta_1}. \quad [35]$$

The frequency of the jth S-spin transition is then given by $J_{IS}\lambda_j$. Note that this definition of the scaling factor differs from that given by Waugh (*6*) in terms of the net rotation angle induced by the pulse sequence. In the current nomenclature there would be two scaling factors for the case of a single IS pair. The difference arises because the present scaling factors give the actual line *positions* in the S-spin spectrum, whereas the single scaling factor as defined by Waugh gives the frequency *difference* between the two parent transitions that occur in the case of a single I spin coupled to S. In multilevel systems there is no convenient generalization of the Waugh scaling factor, and it becomes necessary to plot derivatives of the energy levels of the fictitious Hamiltonian instead (*22*). In the single-spin case we plot the Waugh scaling factor to facilitate comparison with previous work.

A complete description of the decoupling performance would seem to require the construction of the complete two-dimensional energy level surface $\Omega_j(\delta_1, \delta_2)$ as a function of the resonance offsets of I_1 and I_2 for each value of j, followed by partial differentiation with respect to δ_1. This time-consuming calculation is circumvented by taking a single cross section at $\delta_2 = 0$. Sequences performing well over this slice also perform well for any values of δ_1 and δ_2 within their effective bandwidth.

Suppose the decoupling sequence manages to produce a pure scalar operator between the I spins. The S-spin spectrum is particularly easy to predict in this case. The correct eigenstates are the familiar triplet and singlet states with energies $(1/4)J(\delta_1)$ and $(-3/4)J(\delta_1)$, respectively. In the case of a perfect sequence $J(\delta_1)$ is independent of the offset δ_1 and is equal to the unperturbed coupling J. All four S-spin transitions become degenerate and a sharp singlet is observed at the chemical shift of S, corresponding to perfect decoupling.

Although it may seem somewhat surprising to the uninitiated, it is quite possible for a sequence to produce a propagator whose underlying Hamiltonian is a pure scalar operator with a coupling constant that depends on δ_1 (or more generally, on the difference between the chemical shifts of I_1 and I_2). In fact, this is invariably what happens. In such a case the S-spin spectrum consists of two lines with the intensity ratio 3:1 and with positions

$$\frac{1}{4}J_{IS}\frac{\partial J(\delta_1)}{\partial \delta_1}; \qquad \frac{-3}{4}J_{IS}\frac{\partial J(\delta_1)}{\partial \delta_1} \quad [36]$$

corresponding to the S spin evolving in the local field of the triplet or singlet state, respectively. Figure 1 shows this behavior schematically.

We can guess the minimum achievable splitting between these two lines by estimating

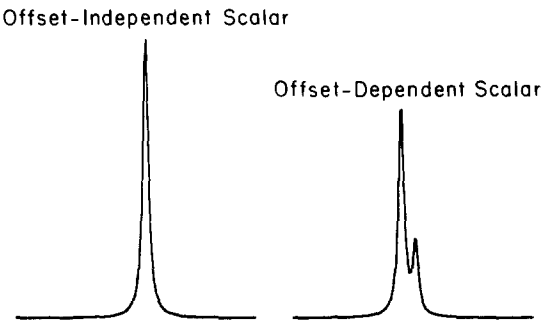

FIG. 1. The expected form of the S-spin spectrum under a decoupling sequence that produces an underlying Hamiltonian that is a pure scalar operator $2\pi J\mathbf{I}_1 \cdot \mathbf{I}_2$. If the effective coupling constant is offset-independent then a sharp singlet is observed. When the coupling constant is offset-dependent a 3:1 pattern emerges, in which the S spin experiences the local field of the triplet or singlet states, respectively.

the minimum rate of change of J with δ_1 for a certain decoupling field amplitude ω_2. During each single pulse of the complicated sequence, the spins I_1 and I_2 precess about their effective fields in the rotating frame. The angle θ between the effective fields remains constant throughout and, assuming $\delta_2 = 0$, is given by

$$\theta = \tan^{-1}(2\pi\delta_1/\omega_2). \qquad [37]$$

Since ω_2 is fixed for the sequences we are considering, the angle θ is constant throughout the sequence: changing the phase of the RF field changes both effective fields in exactly the same way. If the decoupling sequence functions perfectly, all linear and bilinear cross terms are removed, leaving only the projection of I_1 on I_2 intact. As a result the effective Hamiltonian becomes

$$\mathscr{H} = 2\pi J \cos\theta \mathbf{I}_1 \cdot \mathbf{I}_2 \qquad [38]$$

leading directly to a splitting ΔS between the singlet and triplet lines of

$$\Delta S = J_{IS}(2\pi J/\omega_e)\cos\theta \sin\theta, \qquad [39]$$

where ω_e is the effective field felt by I_1:

$$\omega_e = (\omega_2^2 + (2\pi\delta_1)^2)^{1/2}. \qquad [40]$$

When δ_1 is small compared with the RF field amplitude ω_2, Eq. [39] reduces to

$$\Delta S = J_{IS}(2\pi J/\omega_2)(2\pi\delta_1/\omega_2). \qquad [41]$$

For the representative values $J_{IS} = 200$ Hz, $J = 10$ Hz, $\omega_2/2\pi = 2$ kHz, and $\delta_1 = 200$ Hz we find a residual splitting $\Delta S = 0.1$ Hz. The maximum splitting ($\Delta S = 0.385$ Hz) occurs at the offset $\delta_1 = 1414$ Hz, and at $(2^{1/2}/2)\omega_2/2\pi$ for arbitrary ω_2. These rough estimates should be regarded as very optimistic. Most actual decoupling sequences tend to decouple the *two I spins* at a somewhat faster rate as a function of δ_1. That is, the effective coupling constant between the two I spins is smaller than $J\cos\theta$. For some very simple sequences, a detailed evaluation of Eq. [11] predicts a reduction of about $(8/3)^{1/2}$ larger, quite close to the value observed for many of our actual pulse sequences. This larger reduction leads to a larger gradient and larger splitting ΔS for

small δ_1, resulting in poorer performance. As δ_1 approaches the edge of the decoupling bandwidth, the sequence is unable to average away the other operators properly, and the S-spin spectrum breaks up into four lines.

The signature of the aforementioned hypothetical sequence producing a pure scalar operator is shown in Fig. 2 as a function of δ_1 for the case $\delta_2 = 0$. Both the energy eigenvalues and the corresponding λ scaling factors are shown. The triplet state gives rise to a line three times more intense than that from the singlet state. When $\delta_1 = \delta_2 = 0$ there is no residual splitting, but there is a finite residual splitting at all other values of δ_1. This irremovable residual splitting is the direct result of the inability of the sequence to produce a completely offset-independent propagator. We have found no broadband sequence capable of producing a smaller residual splitting near $\delta_1 = 0$, regardless of the degree of iteration, and so regard this estimate as a theoretical lower limit. In contrast to the case of a single I spin, where iterative schemes can produce arbitrarily small residual splittings in the neighborhood $\delta_1 = 0$, two coupled I spins with different chemical shifts result in a small but irremovable residual splitting in the S-spin spectrum.

From Eq. [41] we see that the residual splitting depends on ω_2, and this property carries over to all the sequences we have investigated, whether or not a pure scalar is produced. By contrast, changing ω_2 does *not* change the residual splitting appreciably in the single-spin case as long as the I spin remains within the bandwidth of the decoupling sequence and the flip angles of the pulses are correctly set for each value of ω_2 (5). A simple way to check for the effect of homonuclear coupling is to increase ω_2, adjusting the pulse widths appropriately, while observing the S-spin resonance. If homonuclear coupling is playing a role, the linewidth should decrease. By the same token, RF inhomogeneity gives rise to a superposition of closely spaced multiplets, making the structure difficult to discern.

Cross sections along δ_2 at the point $\delta_1 = 0$ are somewhat more difficult to characterize for practical sequences. Provided δ_2 is within the decoupling bandwidth and a scalar

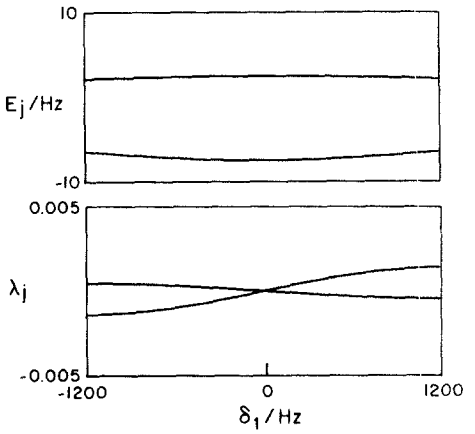

FIG. 2. The energy eigenvalues, E_j, of the Hamiltonian of Eq. [62], assuming an unperturbed homonuclear coupling of 10 Hz and a 2 kHz RF field. The derivatives of the energies, λ_j, shown below, are the scaling factors giving the line positions in the S-spin spectrum.

operator is produced, there will be a residual splitting bounded from below by Eq. [39], in which the angle θ now refers to δ_2 rather than to δ_1. As δ_2 nears the edge of the effective decoupling bandwidth the compensatory properties of the sequence fail and four lines are generally produced in the S-spin spectrum. When δ_2 is much larger than the bandwidth of the sequence, I_1 and I_2 become decoupled and the S-spin spectrum reverts to a sharp singlet. It follows that any additional *heteronuclear* coupling to I_1 has no important role in the proper decoupling of I_1 from S, since I_1 will simultaneously be decoupled from all heteronuclei.

Any real decoupling sequence will produce a mix of other operators in addition to $\mathbf{I}_1 \cdot \mathbf{I}_2$. It is important to assess the influence of these unwanted operators on the S-spin spectrum. As the scalar operator $\mathbf{I}_1 \cdot \mathbf{I}_2$ is approached more closely, the Cartesian product operators become less convenient, and we employ instead the symmetric and antisymmetric linear combinations

$$I_{z+} = I_{1z} + I_{2z} \quad [42]$$

$$I_{z-} = I_{1z} - I_{2z} \quad [43]$$

$$I_{xy+} = I_{1x}I_{2y} + I_{2x}I_{1y} \quad [44]$$

$$I_{xy-} = I_{1x}I_{2y} - I_{2x}I_{1y}, \quad [45]$$

etc. All the symmetric operators $I_{\alpha+}$, $I_{\alpha\beta+}$ commute with $\mathbf{I}_1 \cdot \mathbf{I}_2$ and so can be eliminated by cyclic permutations and phase shifts, in the same way as in the single-spin case. The antisymmetric operators $I_{\alpha-}$, $I_{\alpha\beta-}$ *evolve* under $\mathbf{I}_1 \cdot \mathbf{I}_2$ and can therefore pose problems as the cycle time increases. Fortunately, none of the antisymmetric operators have any nonzero diagonal elements in the eigenbasis of $\mathbf{I}_1 \cdot \mathbf{I}_2$. They also have no nonzero matrix elements connecting the degenerate states within the triplet manifold. If the decoupling sequence produces coefficients for these operators that are small compared to the proton–proton coupling constant the small terms are quenched by J and have very little effect on the decoupling performance. This stabilization of offset-dependent small terms by a larger residual term in the effective I-spin Hamiltonian has been discussed previously for the quadrupolar case (*22*).

PRACTICAL SEQUENCES

It is useless to start with an inferior composite pulse and then attempt to refine away all the errors with the iterative scheme alone. Such an approach misses the point that the *numerical* value of the scalar must be held constant: eliminating all the other operators does not guarantee perfect performance. Ironically, a certain gradient of the scalar part is "built in" during the initial stages, when there are still other terms present in the effective I-spin Hamiltonian. After most of the error terms have been removed it is not possible to alter the numerical value of the scalar much anymore: the effective Hamiltonian, precisely because it is very nearly scalar, becomes invariant to cyclic permutations and phase shifts, and commutes with itself over the various segments of the combined sequence. For this reason, special care must be taken in the design of the composite pulse.

We were able to find suitable composite 180° pulses by using a hybrid approach. Using Eqs. [14]–[21], composite 180° pulses could be discovered which offered com-

pensation for resonance offset and which minimized the production of bilinear cross terms. The composite pulse could then be improved by an exact calculation of its performance over a limited variation of the constituent pulse flip angles, followed by extraction of the underlying Hamiltonian. An improvement was registered whenever the deviation of the scalar part, as a function of offset, was decreased. Using the well-known methods to iteratively improve composite 180° pulses for decoupling sequences by cyclic permutation of 90° pulses (*2–5*) then allowed the bandwidth to be extended without losing the desirable property that the scalar remain as unperturbed as possible. The final stage is then to assemble the decoupling sequence in the form $R\,\bar{R}\,\bar{R}\,R$, which again attenuates the linear and bilinear cross terms without affecting the scalar part much. A selection of the composite 180° pulses we found is set out in Table 3. We distinguish the corresponding decoupling sequences with the label DIPSI-*n*, the index *n* referring to the composite pulse R_n in Table 3. DIPSI stands for "*d*ecoupling *i*n the *p*resence of *s*calar *i*nteractions."

The scaling factors for DIPSI-1, DIPSI-2, and DIPSI-3 are shown in Fig. 3, assuming a 10 Hz proton–proton coupling and a 2 kHz RF field. The scaling factors for WALTZ-16 are included for comparison. Larger bandwidths are offered by the more complex 180°'s. Except for WALTZ-16, the scaling factors show that the underlying Hamiltonian is nearly a pure scalar operator as a function of offset, for the three "triplet" states are nearly degenerate. WALTZ-16 shows the largest deviation from pure scalar behavior, giving a spectrum of four lines over much of the calculated range.

Figure 4 shows the single-spin Waugh scaling factor for WALTZ-16 and each of the DIPSI sequences. The predicted quality of decoupling is extremely good for all these sequences, the scaling factor remaining well below $\lambda = 0.001$ over their respective bandwidths. DIPSI-1 has a cycling rate of 130.4 Hz using a 2 kHz field, and so is comparable to WALTZ-8 in length and complexity. DIPSI-2 and -3 have cycling rates and complexities comparable to WALTZ-16 and WALTZ-32, respectively.

EXPERIMENTAL

Spectra were obtained both on a Bruker AM-400 spectrometer using a standard 10 mm broadband probe and on an AM-500 spectrometer using a 5 mm broadband probe. The 10 mm probe, with its larger sample volume and substantially worse RF homogeneity, provided a searching test of the single-spin bandwidths of the DIPSI

TABLE 3

Phase-Alternating Composite 180° Pulses For Two Coupled Spins $I = \frac{1}{2}$

Label	Sequence	Bandwidth[a]	Length[b]
R_1	$365\ \overline{295}\ 65\ \overline{305}\ 350$	±0.4	1380
R_2	$320\ \overline{410}\ 290\ \overline{285}\ 30\ \overline{245}\ 375\ \overline{265}\ 370$	±0.6	2590
R_3	$\overline{245}\ 395\ \overline{250}\ 275\ \overline{30}\ 230\ \overline{360}\ 245\ \overline{370}\ 340\ \overline{350}$		
	$260\ \overline{270}\ 30\ \overline{225}\ 365\ \overline{255}\ 395$	±0.8	4890

[a] Approximate, in terms of the dimensionless offset parameter $\Delta\omega/\omega_2$.

[b] Total rotation of the composite pulse in degrees.

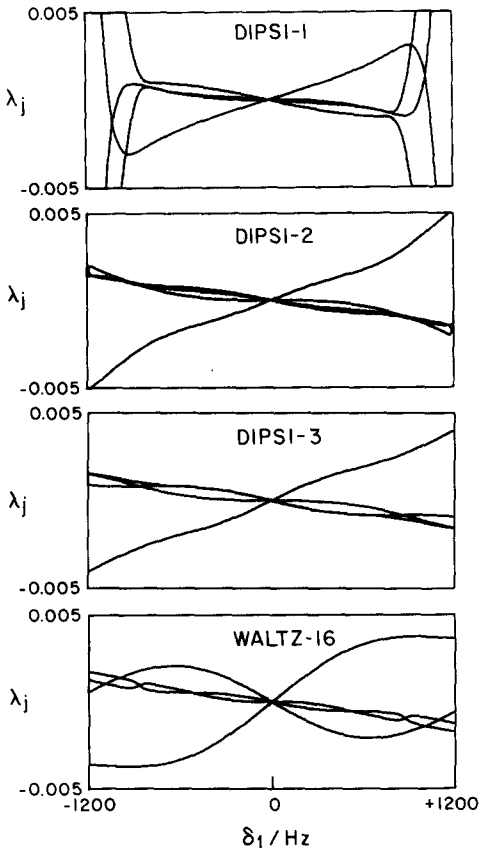

FIG. 3. Scaling factors for DIPSI-1, -2, -3, and WALTZ-16. The scaling factors are shown as a function of δ_1, the offset of the directly coupled I spin, for the case $\delta_2 = 0$, and assuming a homonuclear coupling of 10 Hz and a 2 kHz RF field. Even though the DIPSI sequences use only 180° phase shifts, a pure scalar propagator is approached quite closely. By contrast, WALTZ-16 gives a different signature, showing nonscalar behavior and resulting in four different transitions.

sequences under routine operating conditions. The combination of the 5 mm probe and higher B_0 field available on the AM-500 allowed us to explore the expected fine structure of the carbon-13 resonances due to homonuclear scalar coupling among the protons. An undoped mixture of methyl iodide and ethyl iodide in acetone-d_6 provided one convenient test sample. The width of the carbon-13 resonance of methyl iodide provided an internal standard, and that of the methyl resonance of ethyl iodide revealed the effect of proton–proton coupling. WALTZ-16 and DIPSI-2, since they are of similar length and complexity, should be directly comparable without worrying too much about any differential effects of sample spinning or relaxation (*5*) between the two sequences.

Figure 5 shows the observed 100 MHz carbon-13 resonance (10 mm probe) of methyl iodide (J_{CH} = 151 Hz) as a function of the proton decoupler offset for WALTZ-16, DIPSI-2, and DIPSI-3. As the methyl protons have identical chemical shifts, there

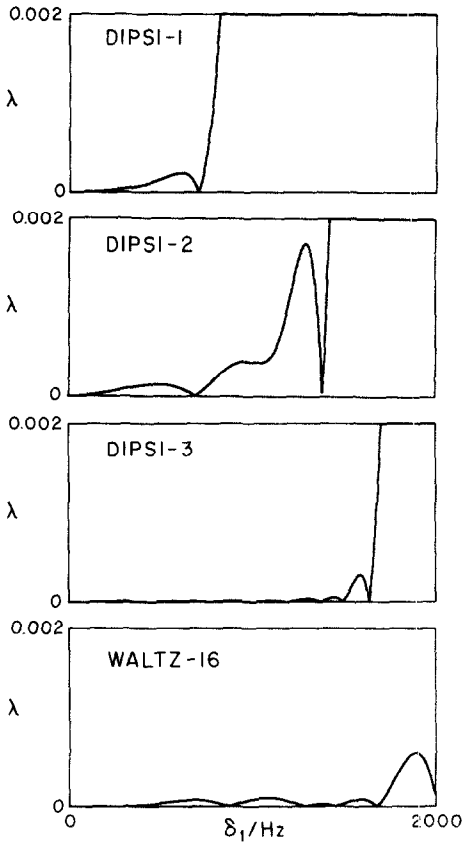

FIG. 4. Single-spin scaling factors for DIPSI-1, -2, -3, and WALTZ-16. All the sequences offer excellent single-spin performance over their bandwidths, but WALTZ-16 gives the largest bandwidth.

is no influence of proton–proton coupling on the heteronuclear decoupling performance. With the sample spinning at 6 Hz, the B_0 field was shimmed until a full width at half-height of 0.20 Hz was obtained using coherent on-resonance decoupling. A sensitivity enhancement function added 0.05 Hz of line broadening, to bring the linewidth to 0.25 Hz. The same settings were retained to investigate the broadband sequences. The carbon-13 signal was not sampled synchronously with the decoupler cycling.

The decoupler field was calibrated and set to the value $\omega_2/2\pi$ = 1480 Hz. This relatively low value provides a stringent test of each sequence. The decoupler offset was incremented in 200 Hz steps over a range ±1400 Hz about exact resonance; a single transient was acquired at each offset. Under these conditions all three sequences give narrow linewidths over their respective bandwidths, and in particular for on-resonance irradiation of the protons. However, WALTZ-16, designed expressly for this single-spin case, gives the largest bandwidth. The observed bandwidths for WALTZ-16 and DIPSI-2 agree well with the theoretical predictions. DIPSI-3 gives an enhanced tolerance to RF inhomogeneity, evident as a slight increase in peak height, but does

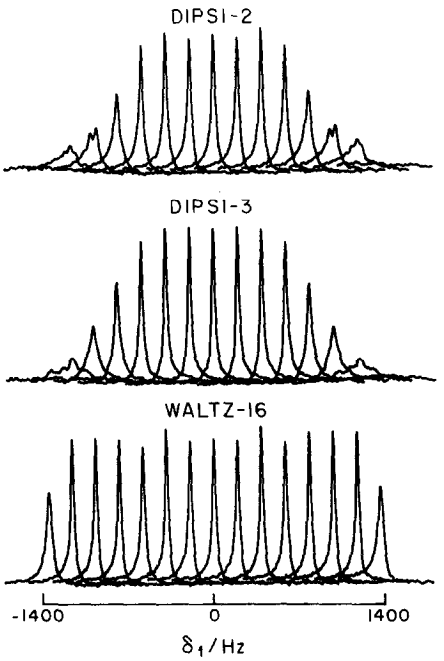

FIG. 5. Carbon-13 resonance of methyl iodide showing the offset dependence of DIPSI-2, DIPSI-3, and WALTZ-16. The decoupler offset has been stepped in 200 Hz increments over a ±1400 Hz range about exact resonance. All three sequences give narrow resonances over their bandwidths, but WALTZ-16 decouples over the largest range. The variations in peak height are attributable to poor ω_2 homogeneity over the sample volume.

not improve much on DIPSI-2 in terms of bandwidth. The cycling rate for DIPSI-3 is only 27.2 Hz under these conditions and is one factor causing the discrepancy between theory and experiment (*5*).

The situation is completely different when there are coupled protons, as there are in most molecules of interest. Figure 6 shows the 125 MHz carbon-13 methyl resonance (5 mm probe) of ethyl iodide in a mixture of methyl and ethyl iodide under conditions of broadband proton decoupling, using decoupling fields of 1100, 1460, and 1930 Hz and a spinning rate of 15 Hz. The decoupler offset was adjusted to the resonance frequency of the methyl protons of ethyl iodide; the methylene protons are then off resonance by 690 Hz. The value of J_{HH} is 7 Hz. Each spectrum is the result of 64 transients; no line broadening has been applied. Coherent on-resonance decoupling gave a linewidth of 0.20 Hz for methyl iodide.

Using WALTZ-16, a very broad multiplet is obtained at $\omega_2/2\pi$ = 1100 Hz. Some line narrowing is achieved with a 1460 Hz field, and a 1930 Hz field narrows the resonance further, but a lineshape approaching a singlet is never obtained. The bizarre "wings" in the lineshape, most apparent at the intermediate field strength, are not artifacts due to poor homogeneity of the static magnetic field B_0. They result from the outer lines of the methyl quartet, which experience an effective heteronuclear

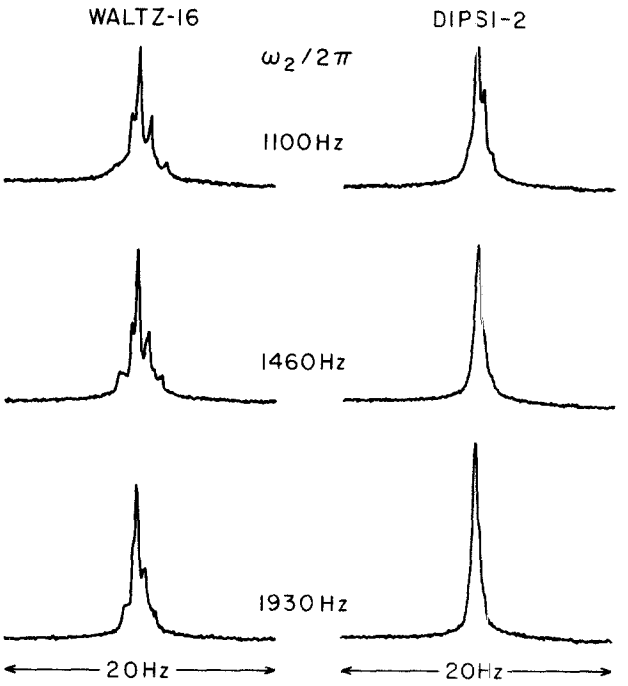

FIG. 6. Carbon-13 methyl resonance of ethyl iodide using three different values of ω_2. Due to the effect of scalar coupling between the protons, distorted lineshapes are obtained with WALTZ-16 (left-hand spectra). DIPSI-2 gives better results, as shown on the right.

coupling constant three times as large as the inner lines (*23*) and which are three times more sensitive to RF field inhomogeneity (*24*).

By using the sequence DIPSI-2 instead, a substantial improvement is obtained, as shown by the right-hand series of spectra. At the lowest field strength of 1100 Hz there is a resolved residual splitting, and some evidence of the pedestal from the outer lines, but the performance is already as good as that obtained with WALTZ-16 at the highest field strength tested. The multiplet pattern shows that a propagator close to a pure scalar operator is being produced by DIPSI-2. At the intermediate value of 1460 Hz the splitting becomes unresolved, showing only as a slight shoulder on the lineshape. With the highest level of 1930 Hz the line narrows still more to give a slightly distorted singlet. Aside from the more pleasing lineshape, DIPSI-2 gives an increase in peak height, and hence carbon-13 sensitivity, of about 25% in this example.

Figure 7 shows the low-field carbon-13 ethylenic resonance of *trans*-cinnamic acid, a molecule previously used to illustrate the effect of homonuclear coupling on broad-band decoupling (*13*). The ethylenic protons form an almost isolated two-spin system with J_{HH} = 16 Hz, providing an ideal test for the effects of proton–proton coupling. The decoupler offset was once again adjusted to the resonance frequency of the directly attached proton. The other proton is then off resonance by −584 Hz. At $\omega_2/2\pi$ = 1100 Hz, WALTZ-16 gives a broad multiplet with the predicted pattern of four lines. DIPSI-

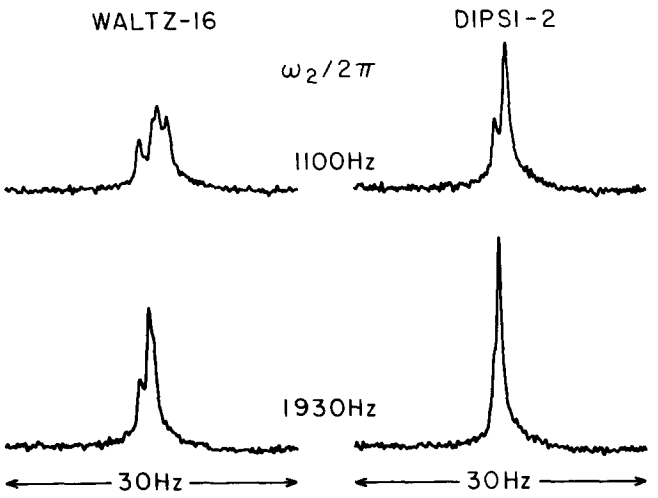

FIG. 7. Low-field ethylene resonance of *trans*-cinnamic acid under conditions of broadband decoupling. WALTZ-16 gives broad multiplets, and at the lowest decoupler level all four lines are resolved. DIPSI-2 narrows the resonance considerably, resulting in better sensitivity and resolution.

2 gives a 3:1-type pattern, almost twice as narrow and twice as intense, under the same conditions. Once again, increasing the field strength to 1930 Hz narrows the resonance line in each instance, but there is still a 50% increase in peak height using DIPSI-2. We have obtained similar results with DIPSI-3. In Fig. 8 we show that the main features of the multiplet patterns, using both WALTZ-16 and DIPSI-2, can be reproduced by simulation even though the latter assumes a perfectly homogeneous RF field.

CONCLUSIONS

Past improvements in broadband decoupling aimed to improve the bandwidth for a given value of ω_2, and much progress has been made. For the single-spin case, sequences like WALTZ-16 deliver very high quality decoupling over bandwidths $\pm\Delta\omega/\omega_2$, and larger bandwidths can be attained if the quality is allowed to deteriorate to some extent (5). While very wide bandwidths may look impressive on paper, they usually offer no particular advantage for proton decoupling and so are not much used. The lowest value of the decoupling field that can be used is dictated by the requirement that the modulation sidebands in the carbon-13 spectrum be acceptably small, so that values much less than 2 kHz are rarely employed. Well-designed probes can achieve fields $\omega_2/2\pi = 3$ kHz with acceptable sample heating. Consequently, for all except the very highest B_0 fields, the entire proton chemical-shift range is decoupled with sequences like WALTZ-16. Furthermore, many molecules do not have proton resonances that span the entire 10 ppm range. In these cases, further improvement in bandwidth is beside the point.

We have shown here that scalar coupling among the protons can also set a lower limit to the decoupling field that can be used and, using WALTZ-16, values substan-

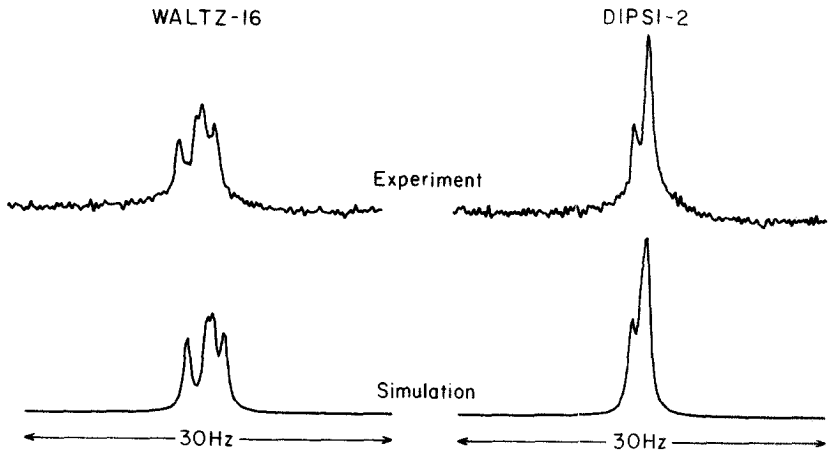

FIG. 8. Comparison between simulation and experiment for *trans*-cinnamic acid using WALTZ-16 (left) and DIPSI-2 (right). The parameters used in the simulation are $\omega_2/2\pi$ = 1100 Hz, δ_1 = 0 Hz, δ_2 = −584 Hz, $^1J_{CH}$ = 150 Hz, $^2J_{CH}$ = 0 Hz, and J_{HH} = 16 Hz. The simulations assume a completely homogeneous ω_2 field and have been artificially line broadened to match the linewidths of the experimental spectra. No attempt has been made to fit the experimental spectra using an ω_2 distribution.

tially larger than 2 kHz may have to be employed if the true instrumental linewidth is the desired resolution. In some cases the multiplet patterns could prove confusing, especially if they happen to overlap or if the carbon-13 nucleus is coupled to other heteronuclei. Isotopic substitution of deuterium for protons changes the proton coupling network; some change in the carbon-13 lineshape may be observed in addition to any splittings and isotope shifts. It goes without saying that experiments like INADEQUATE (*25, 26*) can demand the narrowest carbon-13 resonances to achieve the best sensitivity. The advent of less costly computer memory and array processors increasingly allows very fine digitization of even routine survey spectra, while improvements in temperature stability and B_0 homogeneity (*27–29*) have produced impressively narrow carbon-13 linewidths in favorable cases.

In the aforementioned cases it may be possible to improve resolution and sensitivity by using the DIPSI sequences instead of existing single-spin sequences. Using a 2 kHz field, a bandwidth of 2.4 kHz is obtained with DIPSI-2, large enough for all normal applications at B_0 fields up to 200 MHz for protons and for many applications up to 300 MHz. When scalar coupling among the protons is limiting the carbon-13 resolution, DIPSI-2 can offer a factor of two in line narrowing over WALTZ-16 or, equivalently, a fourfold reduction in RF power.

This work has implications for homonuclear Hartmann–Hahn experiments (*8, 11*). In such experiments a broadband decoupling sequence is often used during the mixing period, causing a coherent exchange of magnetization among the protons. Elegant calculations (*30*) suppose that a pure scalar operator determines the evolution during the mixing sequence. While sequences like MLEV-16, WALTZ-16, or MLEV-17 (*31*) suppress the effects of resonance offset to a large extent and undoubtedly result in magnetization transfer, none of them produces a pure scalar operator. In addition,

calculations show that *both* the MLEV sequences are sensitive to small errors in the RF phase shifts, in disagreement with claims in the literature (*31*). We expect the DIPSI sequences to be of potential use in these experiments.

ACKNOWLEDGMENTS

The authors thank Dieter Suter for stimulating discussions concerning fictitious Hamiltonians. This work has been supported by the Director, Office of Energy Research, Materials Science Division of the U.S. Department of Energy under Contract DE-AC03-76SF00098.

REFERENCES

1. M. H. LEVITT, R. FREEMAN, AND T. FRENKIEL, *in* "Advances in Magnetic Resonance" (J. S. Waugh, Ed.), Vol. 12, p. 47, Academic Press, New York, 1982.
2. J. S. WAUGH, *J. Magn. Reson.* **49,** 517 (1982).
3. A. J. SHAKA, J. KEELER, T. FRENKIEL, AND R. FREEMAN, *J. Magn. Reson.* **52,** 335 (1983).
4. A. J. SHAKA, J. KEELER, AND R. FREEMAN, *J. Magn. Reson.* **53,** 313 (1983).
5. A. J. SHAKA AND J. KEELER, *Prog. NMR Spectrosc.* **19,** 47 (1986).
6. J. S. WAUGH, *J. Magn. Reson.* **50,** 30 (1982).
7. K. V. SCHENKER, D. SUTER, AND A. PINES, *J. Magn. Reson.* **73,** 99 (1987).
8. L. BRAUNSCHWEILER AND R. R. ERNST, *J. Magn. Reson.* **53,** 521 (1983).
9. C. J. LEE, D. SUTER, AND A. PINES, *J. Magn. Reson.* **75,** 110 (1987).
10. P. B. BARKER, A. J. SHAKA, AND R. FREEMAN, *J. Magn. Reson.* **65,** 361 (1986).
11. D. G. DAVIS AND A. BAX, *J. Magn. Reson.* **65,** 355 (1985).
12. J. S. WAUGH, *J. Magn. Reson.* **68,** 189 (1986).
13. A. J. SHAKA, P. B. BARKER, AND R. FREEMAN, *J. Magn. Reson.* **71,** 520 (1987).
14. A. J. SHAKA AND A. PINES, *J. Magn. Reson.* **71,** 495 (1987).
15. U. HAEBERLEN AND J. S. WAUGH, *Phys. Rev.* **175,** 453 (1968).
16. W. MAGNUS, *Commun. Pure Appl. Math.* **7,** 649 (1954).
17. P. PECHUKAS AND J. C. LIGHT, *J. Chem. Phys.* **44,** 3897 (1966).
18. R. M. WILCOX, *J. Math. Phys.* **8,** 962 (1967).
19. I. BIALYNICKI-BIRULA, B. MIELNIK, AND J. PLEBANSKI, *Ann. Phys.* **51,** 187 (1969).
20. W. R. SALZMAN, *J. Chem. Phys.* **82,** 822 (1985).
21. M. H. LEVITT AND R. FREEMAN, *J. Magn. Reson.* **43,** 502 (1981).
22. D. SUTER, K. V. SCHENKER, AND A. PINES, *J. Magn. Reson.* **73,** 90 (1987).
23. W. A. ANDERSON AND R. FREEMAN, *J. Chem. Phys.* **37,** 85 (1962).
24. R. FREEMAN, J. B. GRUTZNER, G. A. MORRIS, AND D. L. TURNER, *J. Am. Chem. Soc.* **100,** 5637 (1978).
25. A. BAX, R. FREEMAN, AND S. P. KEMPSELL, *J. Am. Chem. Soc.* **102,** 4849 (1980).
26. A. BAX, R. FREEMAN, AND T. FRENKIEL, *J. Am. Chem. Soc.* **103,** 2102 (1981).
27. A. ALLERHAND, R. E. ADDLEMAN, AND D. OSMAN, *J. Am. Chem. Soc.* **107,** 5809 (1985).
28. A. ALLERHAND AND M. DOHRENWEND, *J. Am. Chem. Soc.* **107,** 6684 (1985).
29. A. ALLERHAND, R. E. ADDLEMAN, D. OSMAN, AND M. DOHRENWEND, *J. Magn. Reson.* **65,** 361 (1985).
30. N. CHANDRAKUMAR, *J. Magn. Reson.* **71,** 322 (1987).
31. S. SUBRUMANIAN AND A. BAX, *J. Magn. Reson.* **71,** 325 (1987).